First results from the Airborne Visible/Infrared Imaging Spectrometer (AVIRIS)

Gregg Vane

Jet Propulsion Laboratory, California Institute of Technology
4800 Oak Grove Drive, Pasadena, California 91109

ABSTRACT

After engineering flights aboard the NASA U-2 research aircraft in the winter of 1986-87 and spring of 1987, extensive data collection across the United States was begun with the Airborne Visible/Infrared Imaging Spectrometer (AVIRIS) in the summer of 1987 in support of a NASA data evaluation and technology assessment program. This paper presents some of the first results obtained from AVIRIS. Examples of spectral imagery acquired over Mountain View and Mono Lake, California, and the Cuprite Mining District in western Nevada are presented. Sensor performance and data quality are discussed, and in the final section of the paper, plans for the future are described.

1.0 INTRODUCTION

The Airborne Visible/Infrared Imaging Spectrometer (AVIRIS) is the second in a series of instruments under development at the Jet Propulsion Laboratory (JPL) leading to an observatory-class high resolution imaging spectrometer aboard the NASA polar orbiting Earth Observing System (Eos) in the mid-1990s.[1] AVIRIS was conceived of as an operational airborne sensor for routine collection of spectral images to provide data essential for developing new methodologies for information extraction from hyperspectral data acquired from space.[2] This new class of data has proven to be of considerable value to a wide range of earth science disciplines, including botany, geology, atmospheric science and remote sensing science.[3, 4] Work with the predecessor to AVIRIS, the JPL-built Airborne Imaging Spectrometer (AIS)[5], has established a broad community of earth scientists who are now positioned to take advantage of the more comprehensive data sets provided by AVIRIS and its spaceborne successors. Many papers published over the past several years on results obtained with data from AIS attest to the utility of imaging spectroscopy in addressing a broad range of earth science problems.

A thorough description of AVIRIS, its calibration and the AVIRIS ground data processing facility can be found in the papers in these proceedings (see, for example, Porter and Enmark[6], Vane et al.[7], and Reimer et al.[8]). The characteristics of AVIRIS are summarized briefly here. The sensor acquires images from the NASA U-2 aircraft in the whisk-broom imaging mode. Foreoptics consisting of a two-faceted scan mirror and other relay mirrors focus light from one ground instantaneous field of view (GIFOV) onto four optical fibers, as shown in Figure 1. Each fiber terminates in one of four spectrometers, where the light is dispersed off an aspheric grating and focussed onto a line array of detectors. Figure 2 is an artist's rendering of the flight hardware, showing the physical layout of the instrument's major components. Spectrometer A has a 32-element line array of silicon detectors and covers the spectral range 0.40 to 0.71 μm; Spectrometers B, C, and D each have a 64-element line array of indium antimonide detectors and cover the spectral ranges 0.68 to 1.28, 1.24 to 1.86, and 1.83 to 2.45 μm, respectively. Each picture element (pixel) on the ground is imaged in 220 spectral bands. After resampling to equalize the spectral sampling interval and remove the overlap between spectrometers, this reduces to 210 spectral bands in the radiometrically calibrated data.[7] In each cycle of the foreoptics scan mirror, 614 cross-track pixels are acquired. Twelve scans per second are made as the forward motion of the aircraft provides the along-track scan. Each pixel is 20 by 20 m at sea level from the nominal altitude of the U-2, with a pixel-to-pixel center spacing of 17 m to minimize spatial undersampling over mountainous terrain. The oversampling is corrected during geometric rectification of the data at the AVIRIS ground data processing facility. The result is an image 550 pixels wide, spanning 10.5 km on the ground. On board the aircraft, the raw data are digitized to 10 bits and recorded on a high-density tape recorder at the rate of 17 Mbps. An onboard calibrator provides a frequent update of the detector dark current and instrument spectral and radiometric performance. The observational characteristics of the AVIRIS system are summarized in Tables 1, 2, and 3.

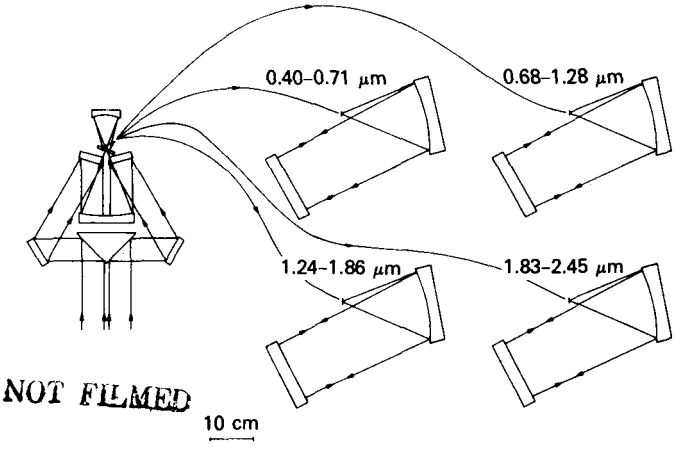

Figure 1. Schematic diagram of the AVIRIS optical configuration.

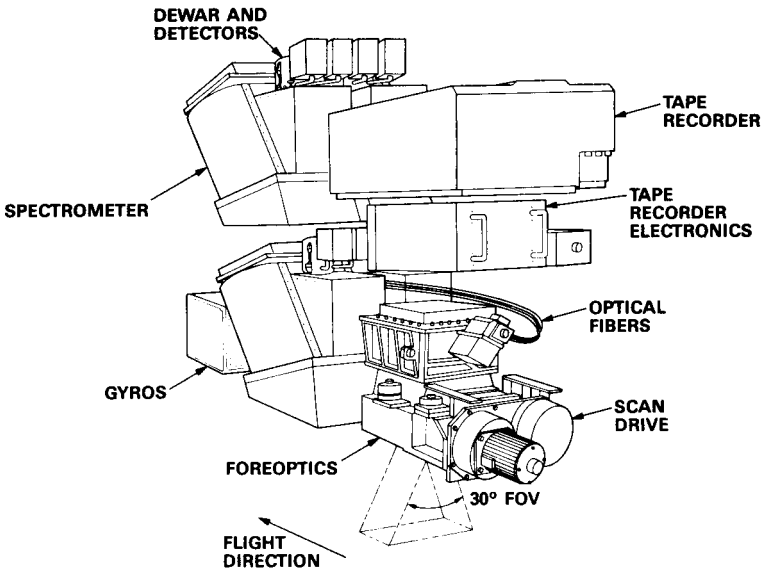

Figure 2. Artist's drawing of the AVIRIS flight hardware showing the physical layout of the major subsystems.

Table 1. General Performance of AVIRIS

Parameter	Performance
Spectral Coverage	0.40 to 2.45 μm
Spectral Sampling Interval	9.6 to 10.0 nm
Number of Spectral Bands	
Raw Data	220
Radiometrically Corrected Data	210
Instantaneous Field of View (IFOV)	0.95 mrad
Ground IFOV from U-2 Aircraft	20 m
Angular Field of View (FOV)	30 deg
Ground FOV from U-2 Aircraft	10.5 km
Number of Cross-Track Pixels	
Raw Data	614
Geometrically Corrected Data	550
Data Encoding	10 bits
Data Rate	17 Mbps
Radiometric Calibration Accuracy (Laboratory)	
Absolute	7.3%
Spectral Band-to-Band	0.4%
Spectral Calibration Accuracy	2 nm

Table 2. Required and Achieved Performance of AVIRIS Scanner

Parameter	Required	Achieved
Scan Rate	12 Scans/sec	12 Scans/sec
Cumulative Pixel Position Error over 1 Scan Line	0.5 Pixel	0.26 Pixel
Maximum Pixel-to-Pixel Position Error within 1 Scan Line	0.1 Pixel	0.06 Pixel
Uncompensated Motion of Scan Drive Housing due to Vibration	0.1 Pixel	0.01 Pixel

Table 3. AVIRIS Signal-to-Noise Performance in the Laboratory

Spectrometer	Wavelength (μm)	Required SNR	Measured SNR[a]
A	0.7	100:1	150:1
B	1.0	None	140:1
C	1.6	None	70:1
D	2.2	50:1	30:1

[a] The measured performance is from integrating sphere data normalized to a scene (ground) albedo of 0.5 through a standard mid-latitude, mid-summer atmosphere with 23-km visibility.

Acquisition of data with AVIRIS for scientific applications began in June 1987 and continued through the middle of October 1987, when the instrument was returned to JPL for a post-season calibration and instrument upgrades. Data were acquired over vegetated sites in Florida, Minnesota, Oregon and California, over the ocean off the California coast near San Francisco, and over geological sites in Colorado, Wyoming, Utah, Nevada, Arizona and California. Also, data were collected over a radiometric calibration site in the Mojave Desert of California. Most of the flight activity in 1987 was done in support of the NASA-sponsored AVIRIS data evaluation and technology assessment program, although several investigators were funded outside this program by NASA to conduct basic earth science research. During the course of the summer, data were acquired for a total of 20 investigators. In the following section of the paper, early results from three of the sites under study by the AVIRIS project are presented.

2.0 FIRST RESULTS FROM AVIRIS

AVIRIS is flown in the NASA U-2 aircraft from the Ames Research Center at Moffett Field, California. Because of the proximity to the San Francisco peninsula with its varied cultural and natural surface features, the first images acquired with AVIRIS were from that area. Figure 3 shows a suite of four spectral images acquired over the Moffett Field and Mountain View areas in June 1987 at the start of scientific data acquisition. Shown are raw data to which no radiometric or geometric corrections have been applied except for an onboard roll correction performed during image acquisition. Figure 3(a) is from Spectrometer A, spectral band 30, centered at 0.682 μm; Figure 3(b) is from Spectrometer B, spectral band 68, centered at 1.014 μm; Figure 3(c) is from Spectrometer C, spectral band 125, centered at 1.518 μm; and Figure 3(d) is from Spectrometer D, spectral band 188, centered at 2.095 μm. The images are 614 pixels across and 512 lines in length. One scan line of 614 pixels is acquired in one twelfth of a second; 512 scan lines are acquired in about 43 seconds. Figure 3 represents a small portion of a much longer flight line beginning at Point Reyes, north of San Francisco, and extending south to San Jose, which is a few kilometers south of Mountain View. The total flight line length was over 100 km, which represents about 7 minutes of data acquisition.

A visual inspection of the images in Figure 3 reveals several characteristics of the quality of the AVIRIS data. The inherent geometry of the raw images is good, as evidenced by the straight runways at Moffett Field and other linear features in the scene. The stability of the detector output on a time scale from one twelfth of a second to 43 seconds is also good, as can be seen by the uniformity of the images. Indeed, over the entire 7 minutes of the total flight line over the San Francisco area, the detector output appeared to be stable, except for the offset in the spectral images from Spectrometer D, discussed below. The spatial resolution appears to match the performance expected from laboratory measurements of the instrument instantaneous field of view. For example, the dikes separating the evaporation ponds to the east of Moffett Field are 15 to 20 meters wide; the AVIRIS pixel size from the 20 km altitude of the U-2 is 20 m. The dikes are clearly visible in

(a)

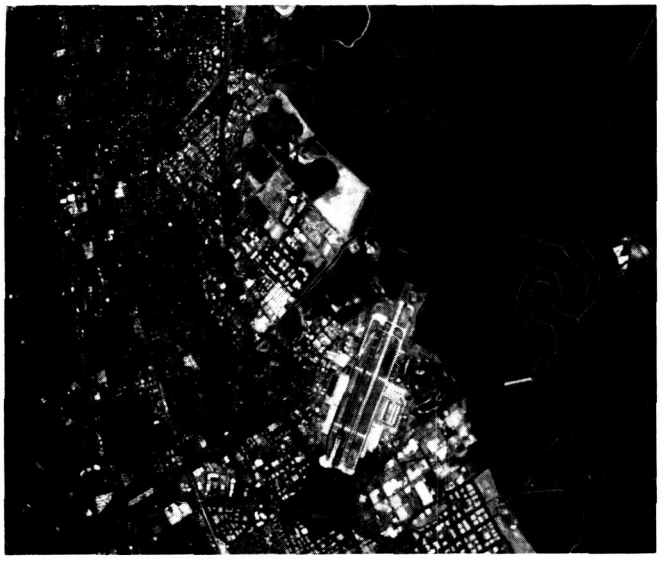

(b)

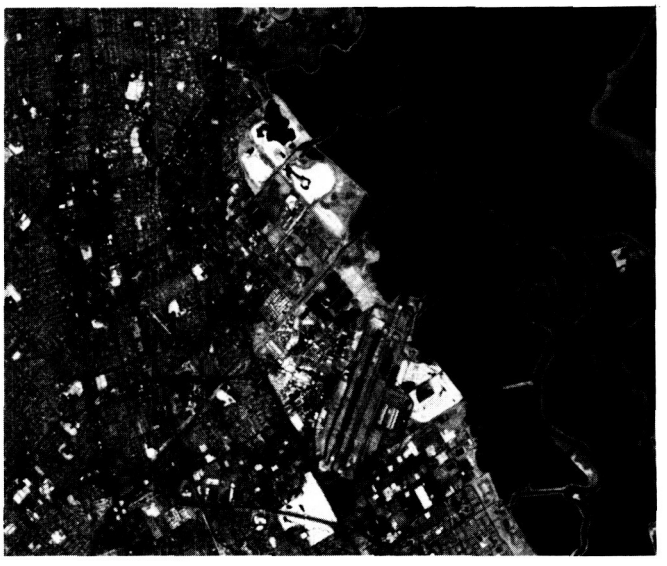

(c)

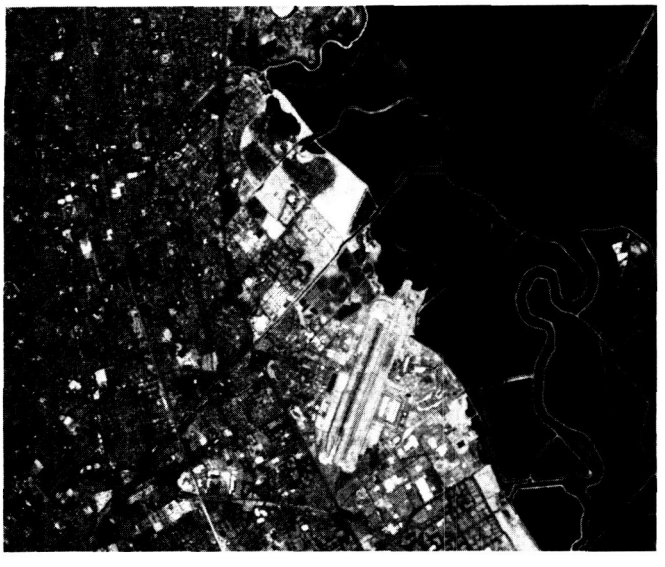

(d)

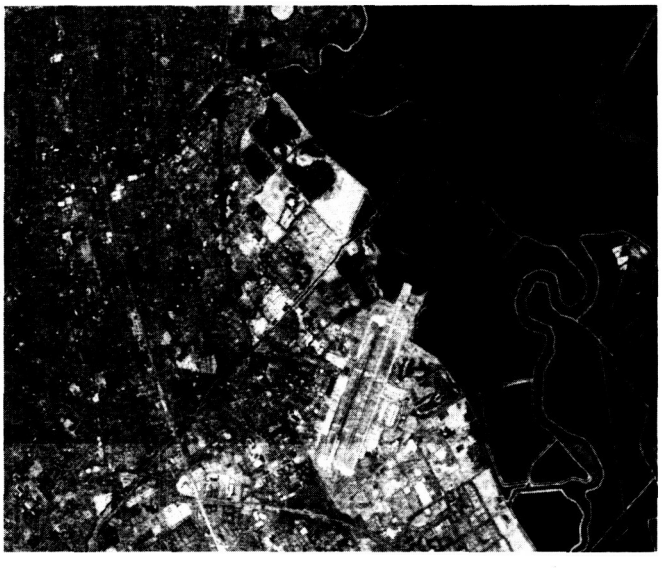

Figure 3. Four 10-nm spectral images from Mountain View, California, each from a different AVIRIS spectrometer: (a) image A is from spectrometer A, spectral band 30, centered at 0.682 μm; (b) image B is from spectrometer B, spectral band 68, centered at 1.014 μm; (c) image C is from spectrometer C, spectral band 125, centered at 1.518 μm; and (d) image D is from spectrometer D, spectral band 188, centered at 2.095 μm. These images are from raw data; no radiometric or geometric correction has been applied except for aircraft roll compensation performed during data acquisition. In addition to these four images, another 216 10-nm images across the spectral range from 0.40 to 2.45 μm were acquired simultaneously.

the images in Figure 3, appearing as thin, dark features (the tops of the dikes) outlined on either side by bright lines (the salt deposits on the flanks of the dikes). The visual appearance of the images also indicates the range in signal-to-noise ratios (SNRs) among the four AVIRIS spectrometers. The SNRs measured in the laboratory for spectral bands 30 and 68 are in excess of 100:1 for a surface albedo of 0.5, for spectral band 125 about 70:1, and for band 188 about 30:1. Figure 3(d) exhibits one of the artifacts of the AVIRIS electronics characteristic of the instrument configuration during the 1987 flight season. The offset in brightness occurring near the bottom of the image is the result of a vibrationally induced change in a potentiometer setting in the preamplifier circuit, which caused a step change in the offset applied to the data during onboard processing. In addition to this non-subtle effect occurring most frequently in Spectrometer D, at the end of the flight season it was discovered that a long-term drift in the setting of the same potentiometer caused a variation in the overall signal level that, while not obvious from a visual inspection of the images, has an effect on instrument radiometry. This effect appears throughout all four spectrometers to varying degrees during the flight season. The cause of the problem will be removed during instrument refurbishment in the winter of 1987-88.

A color rendition of the Moffett Field image is shown in the frontispiece to the Proceedings. Using radiometrically corrected data, the image was produced from three 0.01 μm wide spectral bands centered at 0.557, 0.665, and 0.910 μm. These spectral bands were assigned the colors blue, green, and red, respectively. In this rendition, red corresponds to healthy vegetation and blue/green corresponds to water. Note the degree of shading in the water in the southern part of San Francisco Bay and in the evaporation ponds to the east of Moffett Field. This shading is indicative of variations in the concentration and composition of suspended particulates in the water. The Moffett Field data set has been archived at JPL as one of two standard products available to investigators wishing to gain experience in working with AVIRIS data. The second data set, described below, is from Cuprite, Nevada. A copy of either data set can be obtained by writing to the author.

Figure 4 shows another image acquired with AVIRIS in the first flight season. Shown is an image in spectral band 68 (1.014 μm) of Mono Lake, California. Mono Lake is an extinct volcanic caldera some 15 km in diameter, located at about 2500 m above sea level. It provides a good test of instrument performance because of the very high albedo contrast between the dark water and the bright evaporite deposits on the islands and along the shores of the lake. The north shore of the lake is characterized by broad, contiguous beaches of seasonal bright evaporite crust and dark basalt pebbles that extend with more or less lateral continuity an arcuate distance of 15 km. Visual inspection of the image indicates that the boundaries between these high contrast areas remain sharp, verifying that AVIRIS does not suffer from the effects of residual imagery which result from inefficient charge transfer during detector readout, and from such optical effects as stray light. The image also attests to the large dynamic range of the sensor. Details in the image are clear over a wide range of surface brightnesses. Note the thin, filamentous cumulus cloud over the lake.

Figure 5 is an image acquired over the Cuprite mining district in western Nevada; shown is spectral band 68, centered at 1.014 μm. The mining district straddles U.S. Highway 95 approximately 30 km south of Goldfield, Nevada. The eastern half of the district is an area of extensive hydrothermal alteration within a sequence of rhyolitic welded ash flow and air fall tuffs. The altered units consist of a central core of almost pure silica, a ring of opalized rocks containing alunite and kaolinite, and an outer argillized zone containing mainly kaolinite, montmorillonite, and opal, and some limonite.[9] Cuprite has been studied extensively over the past 10 years with almost every remote sensing instrument operating in the wavelength region between 0.4 and 14 μm.

Using the Spectral Analysis Manager (SPAM) software developed at JPL[10], spectra were constructed after radiometric calibration of the data from the areas indicated in Figure 5. Area "A" is the Stonewall Playa. A representative spectrum obtained from the average of a 5 by 5 pixel portion of the playa is shown in Figure 6. The spectrum has the characteristic shape of the solar irradiance curve convolved with the absorption spectrum of the earth's atmosphere. The major absorption features at 1.4 and 1.9 μm are due to atmospheric water. Using the wavelength position mapping feature of SPAM, many of the smaller atmospheric absorption features were located in terms of their wavelength positions in the AVIRIS data. The first number associated with each identified feature in Figure 6 was obtained from the AVIRIS data in this manner. The information in parentheses indicates the wavelength position of the feature according to the LOWTRAN VI atmospheric model, and the atmospheric constituent(s) causing it. As can be seen, there is very good agreement between the AVIRIS-derived and LOWTRAN wavelength positions. Note the CO_2 absorption features at 1.58 and 1.61 μm. These features are separated by only 0.03 μm, but are clearly resolved at the AVIRIS spectral sampling level, indicating that the spectral resolution of the instrument as defined by the Nyquist sampling theorem is being realized. According to the Nyquist theorem, a spectrum sampled at 0.01 μm intervals is sampled at a spectral resolution of 0.02 μm.

Figures 7, 8, and 9 show spectra from areas B, C, and D, respectively, in Figure 5. The spectra were constructed after dividing the Cuprite scene by the spectrum in Figure 6 to correct for atmospheric and solar insolation effects. Area B is known locally as Kaolinite Hill for its extensive and well-exposed deposit of the clay mineral kaolinite. The wavelength positions of the absorption features were determined using the SPAM software and agree closely with the laboratory-determined wavelength positions for these features.[11, 12] The identification of the double absorption feature at 2.16 and 2.21 μm was one of the major criteria in specifying the spectral and radiometric resolution of AVIRIS. Through analysis of AIS spectra from Kaolinite Hill and laboratory spectral analysis, it was determined that a SNR of about 50:1 is required to resolve the double absorption feature at the AVIRIS spectral resolution. As noted earlier in the paper, the SNR of AVIRIS at this wavelength during the 1987 flight season was only 30:1. The feature has been resolved nonetheless because of the excellent exposure of the mineral at Cuprite.

Other minerals at Cuprite which are difficult to distinguish from kaolinite visually are alunite, whose spectrum is shown in Figure 8, and Buddingtonite, whose spectrum is shown in Figure 9. Alunite occurs widely throughout the Cuprite area, while Buddingtonite has been observed only in a few locations at the site. The occurrence of Buddingtonite at Cuprite was discovered only in 1985 through the analysis of AIS spectra.[13] Its occurrence there represents the fifth known location for the mineral in a hot spring environment, where it is associated with disseminated gold deposits. The absorption features at 2.02 and 2.11 μm are its chief diagnostic features distinguishing it spectrally from the other minerals at Cuprite. Alunite is distinguished by its absorption feature at 2.16 μm, which, at the spectral resolution of AVIRIS, is resolved as a double absorption feature. The secondary feature occurs at 2.20 μm.

3.0 FUTURE PLANS

During the course of instrument checkout and calibration prior to the start of data collection with AVIRIS in the summer of 1987, several areas of less-than-optimal performance were identified and an upgrade program was planned for the period between the 1987 and 1988 flight seasons. A performance deficiency related to changes in offset has been discussed in this paper. Thermally induced drift in signal levels resulting from distortion of the spectrometer alignment, and an 8 percent vignetting on the left side of the foreoptics were also discovered. Further, a small amount of systematic noise in Spectrometer D, and random noise in both Spectrometer C and D resulted in lower SNRs than the instrument model predicts should be achievable in these spectrometers. Aside from the lower SNR performance, the net effect of most of the deficiencies is a degradation in the absolute radiometry of the data. To remove these performance-limiting factors and place the sensor in its final configuration for long-term operations, the following activities will be conducted in the winter of 1987-88. After a complete post-flight-season spectral and radiometric calibration of AVIRIS, the instrument will be disassembled for rework. To remove the offset drift and minimize the random and periodic electronic noise, the preamplifier and clock driver board designs will be modified and new boards fabricated. To remove vignetting in the foreoptics, the optics will be realigned. The thermally induced drift in signal level will be addressed by (1) implementing a new spectrometer heater design, and (2) floating the spectrometers on kinematic mounts. The latter should also minimize the effects of the vibrational environment. A few other small tasks will be completed during this winter that will improve the reliability of the sensor for long-term operations.

Figure 4. Raw AVIRIS image of Mono Lake, California, in spectral band 68, centered at 1.014 μm. No radiometric or geometric correction has been applied. The scene is approximately 10.5 by 20 km in area.

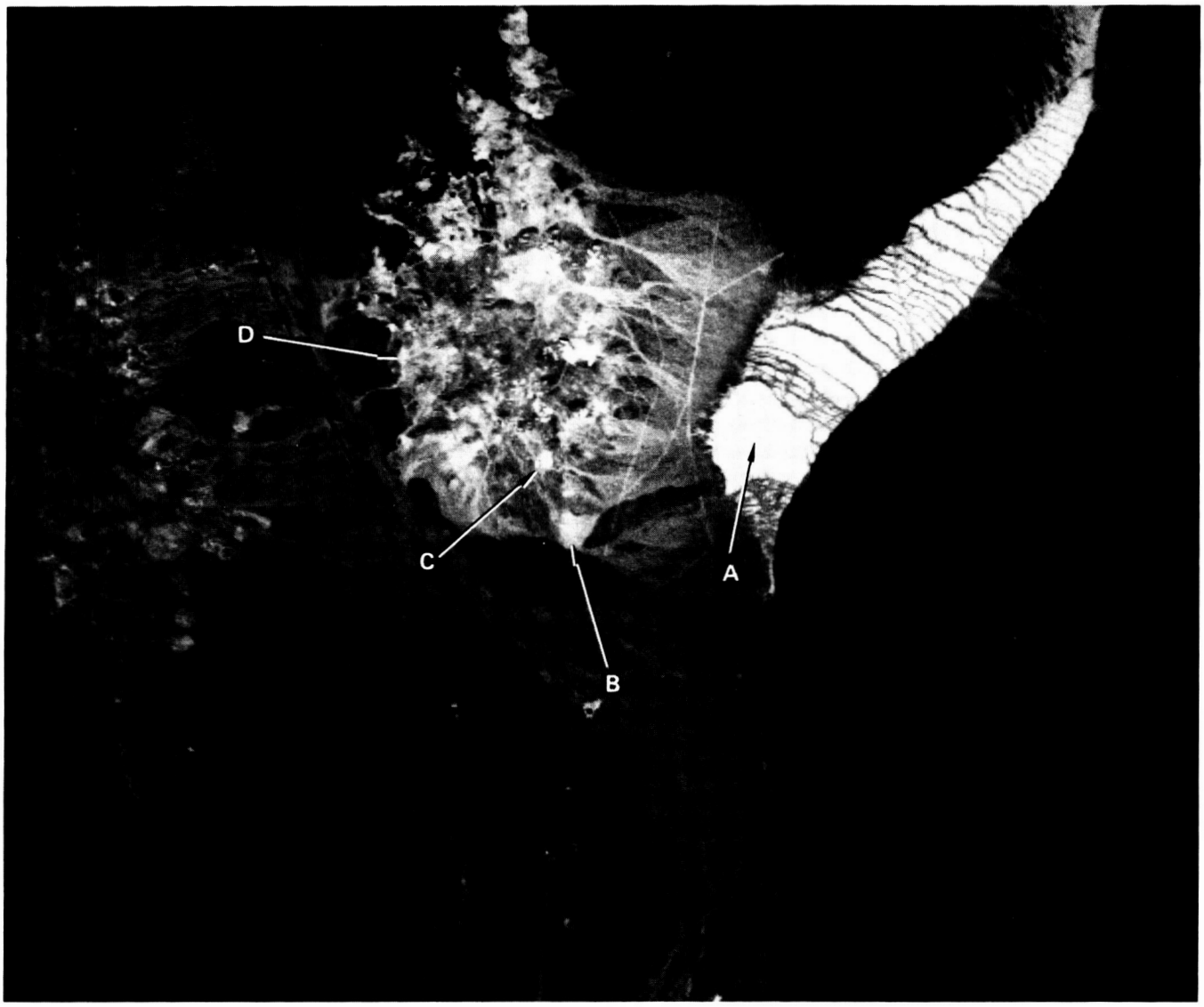

Figure 5. AVIRIS image of the Cuprite mining district, Nevada, in spectral band 68, centered at 1.014 μm. A is Stonewall Playa, B is Kaolinite Hill, C marks the location of a deposit of the mineral alunite, and D marks the location of a deposit of the mineral Buddingtonite.

In addition to the upgrades to the instrument, further work is planned in the areas of data processing and instrument calibration. Results from further analysis of flight data will be used to determine whether additional efficiency can be achieved at the ground data processing facility by reducing some of the steps involved in the application of the radiometric calibration to the flight data. Further analysis of the procedures used in the laboratory for obtaining the data for the radiometric calibration file will be conducted to determine if additional calibration accuracy can be achieved. Field experiments to check the spectral and radiometric calibration of AVIRIS in the air were conducted in the summer of 1987. Analysis of these data is just beginning. Additional experiments are planned for 1988 to check instrument performance after the upgrades are completed.

NASA is planning a data collection campaign with AVIRIS in 1988 for the atmospheric science, botany, geology, hydrology, oceanography, and remote sensing science communities. Part of the work in 1988 will be the completion of the data evaluation and technology assessment program begun in 1987. The remainder will be in support of ongoing research in the earth sciences. Data collection in 1988 will take place in the United States and Canada, but future deployments outside North America are already under consideration. AVIRIS is expected to be the major sensor for gathering high spectral resolution imagery across the 0.4 to 2.5 μm region until the launch of the Earth Observing System (Eos) in the mid-1990s. The goal of the AVIRIS project is to collect, process, and distribute consistent, well-calibrated data in support of the earth system science program leading to Eos and beyond.

4.0 ACKNOWLEDGEMENTS

During the past three years, 45 engineers, scientists and support personnel have worked hard at JPL to bring the AVIRIS system to completion. The author would like to express his deep gratitude to all those whose efforts have contributed to the success of this joint endeavor. The work described in this paper was carried out at the Jet Propulsion Laboratory, California Institute of Technology, under a contract with the National Aeronautics and Space Administration.

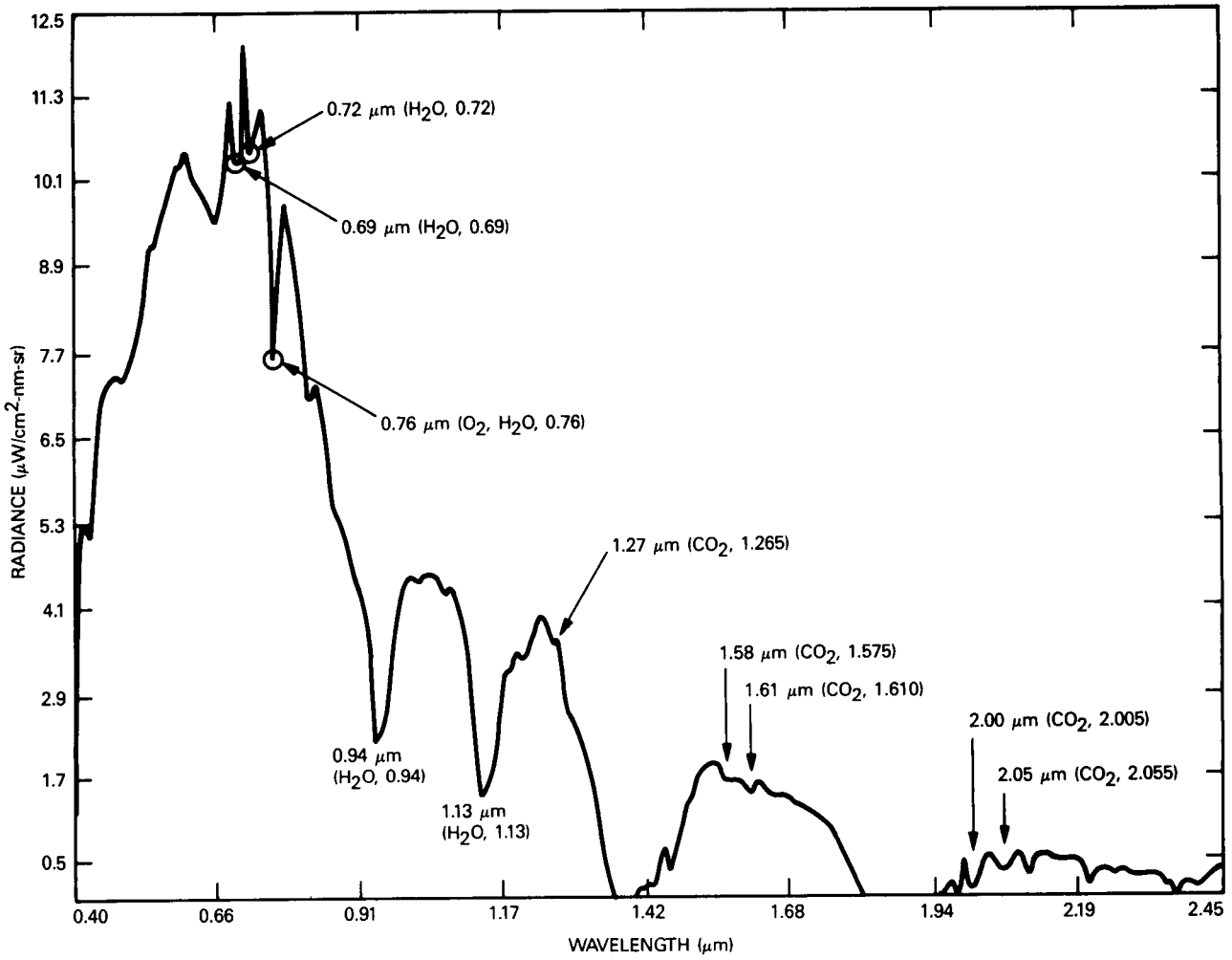

Figure 6. Full spectrum of a 5 by 5 pixel area in the center of Stonewall Playa. The data have been radiometrically corrected as described by Vane et al.[7] The wavelength positions of several atmospheric absorption features are indicated. The first number is derived from the AVIRIS data. In parentheses are the wavelength position of that feature from the LOWTRAN VI atmospheric model, and the atmospheric constituent(s) responsible for it.

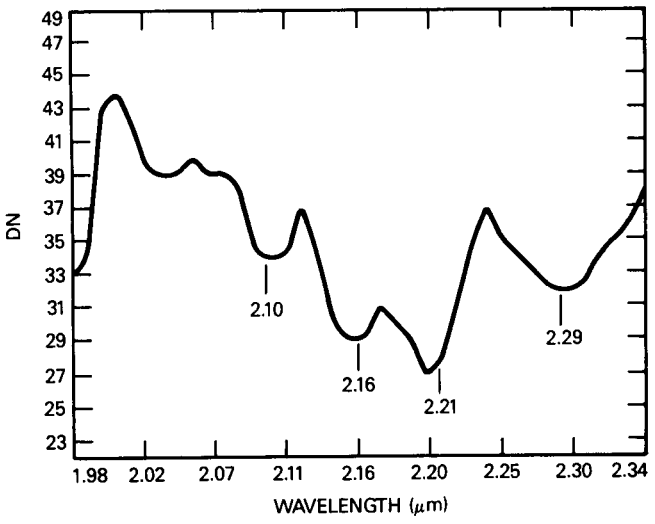

Figure 7. Single pixel spectrum from Kaolinite Hill showing the diagnostic double absorption feature at 2.16 and 2.21 μm due to the OH molecule in the kaolinite crystal lattice. The data were divided by the spectral reflectance curve in Figure 6 to remove the effects of solar insolation and atmospheric absorption.

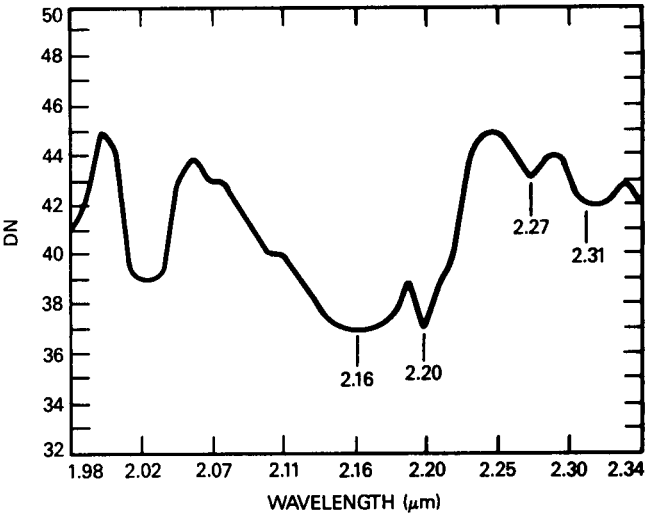

Figure 8. Single pixel spectrum of the mineral alunite from location C in Figure 5. The data were divided by the spectral reflectance curve in Figure 6 and show the diagnostic absorption feature at 2.16 μm resolved into its doublet. The secondary feature is at 2.20 μm.

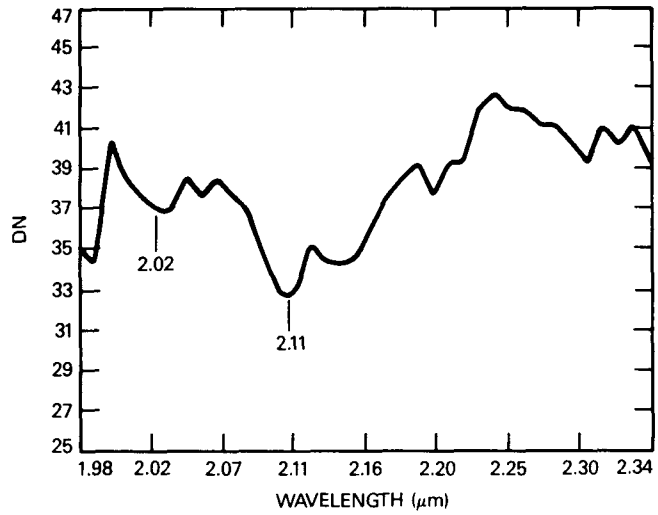

Figure 9. Single pixel spectrum of the mineral Buddingtonite from location D in Figure 5. The data were divided by the spectral reflectance curve in Figure 6. Characteristic absorption features at 2.02 and 2.11 μm identify this mineral.

5.0 REFERENCES

1. A. F. H. Goetz et al., "High resolution imaging spectrometer: Science opportunities for the 1990s," NASA TM 86129(2c) (1987).

2. G. Vane, M. Chrisp, H. Enmark, S. Macenka and J. Solomon, "Airborne Visible/Infrared Imaging Spectrometer: An advanced tool for earth remote sensing," Proc. 1984 IEEE Int'l. Geoscience and Remote Sensing Symposium, SP215, 751-757 (1984).

3. G. Vane and A. F. H. Goetz, "Terrestrial imaging spectroscopy," Remote Sensing of Environment, 24(1), in press (1987).

4. A. F. H. Goetz, G. Vane, B. N. Rock and J. E. Solomon, "Imaging spectrometry for earth remote sensing," Science, 228(4704), 1147-1153 (1985).

5. G. Vane, A. F. H. Goetz and J. B. Wellman, "Airborne Imaging Spectrometer: A new tool for earth remote sensing," IEEE Trans. on Geoscience and Remote Sensing, GE-22(6), 546-549 (1984).

6. W. M. Porter and H. T. Enmark, "A system overview of the Airborne Visible/Infrared Imaging Spectrometer (AVIRIS)," Proc. SPIE, 834 (1987).

7. G. Vane, T. G. Chrien, E. A. Miller and J. H. Reimer, "Spectral and radiometric calibration of the Airborne Visible/Infrared Imaging Spectrometer," Proc. SPIE, 834 (1987).

8. J. H. Reimer, J. R. Heyada, S. C. Carpenter, W. T. S. Deich and M. Lee, "AVIRIS ground data processing system," Proc. SPIE, 834 (1987).

9. M. J. Abrams, R. P. Ashley, L. C. Rowan, A. F. H. Goetz and A. B. Kahle, "Mapping of hydrothermal alteration in the Cuprite mining district, Nevada, using aircraft scanner images for the spectral region 0.46 to 2.36 μm," Geology, 5, 713-718 (1977).

10. A. S. Mazer, M. Martin, M. Lee and J. E. Solomon, "Image processing software for image spectrometry data analysis," Remote Sensing of Environment, 24(1), in press (1987).

11. R. N. Clark, T. King, M. Klejwa, G. A. Swayze and N. Vergo, "High spectral resolution reflectance spectroscopy of minerals," submitted to Jour. Geophysical Res. (1987).

12. C. Inouye, A. F. H. Goetz and S. Schultz, "Reflectance spectra of 156 minerals," JPL Publication in preparation, Jet Propulsion Laboratory, Pasadena, CA (1987).

13. A. F. H. Goetz and V. Srivastava, "Mineralogical mapping in the Cuprite mining district, Nevada," in Proceedings of the Airborne Imaging Spectrometer Data Analysis Workshop, Gregg Vane and Alexander F. H. Goetz, eds., JPL Publication 85-41, Jet Propulsion Laboratory, Pasadena, CA, 22-31 (1985).